

## Supporting Information

### **Observation of Stepwise Ultra-fast Crystallization Kinetics of Donor-Acceptor Conjugated Polymers and Correlation with Field Effect Mobility**

Shaochuan Luo<sup>2,3</sup>, Nan Li<sup>3</sup>, Song Zhang<sup>4</sup>, Chen Zhang<sup>1</sup>, Tengfei Qu<sup>2</sup>, Michael U. Ocheje<sup>5</sup>,  
Gi Xue<sup>2</sup>, Xiaodan Gu<sup>4</sup>, Simon Rondeau-Gagné<sup>5</sup>, Wenbing Hu<sup>2</sup>, Sihong Wang<sup>3</sup>, Chao Teng<sup>1</sup>,  
\*, Dongshan Zhou<sup>2</sup>, \* and Jie Xu<sup>6</sup>, \*

<sup>1</sup>Institute of Marine Biomedicine, Shenzhen Polytechnic, Shenzhen, China

<sup>2</sup>Department of Polymer Science and Engineering, School of Chemistry and Chemical Engineering,  
Shenzhen R&D Center, State Key Laboratory of Coordination Chemistry, Key Laboratory of High  
Performance Polymer Materials and Technology MOE, Nanjing University, Nanjing, China

<sup>3</sup>Pritzker School of Molecular Engineering, University of Chicago, Chicago, IL 60637, USA

<sup>4</sup>School of Polymer Science and Engineering, Center for Optoelectronic Materials and Devices,  
University of Southern Mississippi, Hattiesburg, MS, USA

<sup>5</sup>Department of Chemistry and Biochemistry, University of Windsor, Windsor, Ontario, Canada

<sup>6</sup>Nanoscience and Technology Division, Argonne National Laboratory, Lemont, IL, USA

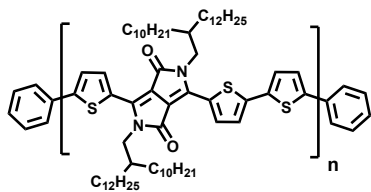
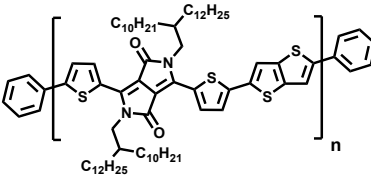
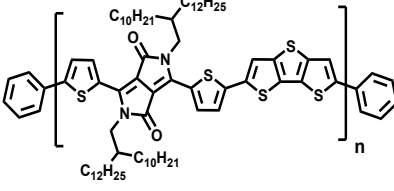
## Discussion

Correlation between crystallization of bulk sample and the crystallization of film solidified from solution

From the FSC study on the melt crystallization of bulk solid polymers, we learned that the crystallinity can be improved by pre-exist/formed crystallites. Based on these observations, we infer that the existing of pre-formed aggregates (nanocrystallites) in solutions may enhance the crystallization of DPP-based polymers during solidification.

In experiments, we found similar stepwise crystallization behavior with two melting peaks in both bulk sample and solution-processed film samples. (1) In the crystallization study of bulk sample (Fig. R4 left, Figure 2d in the manuscript), we observe two melting peaks. The high-T peak, which relates to the melting of H-crystallites, shows no change with the annealing time while the low-T peak gradually increases and shifts to higher temperature with the annealing time due to the perfection of crystals. In the study of the solution-processed films (Fig. R4 right, Figure 5a in manuscript), two melting peaks and similar crystallization behaviors are observed too. The melting temperature of high-T peak shows no change with different pretreatments and post-annealing processes while low-T peaks increase and shift to higher temperature after annealing in these film samples. (2) In the solution process film, sample with large area high-T peak shows a higher melting enthalpy in the subsequent annealing process. This phenomenon is similar with the promoted crystallinity and crystallization rate of bulk sample with H-crystallites (compare to without crystallites) in the isothermal study. As such, we can infer that the crystallization behavior obtained from bulk crystallization study can be correlated to the crystallization study of solution processed films.

**Table S1.** Physical properties of DPP polymers

Polymer	Chemical structure	$M_n$ (kDa) <sup>a</sup>	$\bar{D}_w$ <sup>b</sup>
DPP-T		47	2.83
DPP-TT		51	3.62
DPP-TTT		17	3.21
DPP-TTT		26	3.69
DPP-TTT		44	2.32

<sup>a</sup> Number-average molecular weight measured by high temperature GPC using trichlorobenzene as eluent at 170 °C. <sup>b</sup> Weight dispersity.

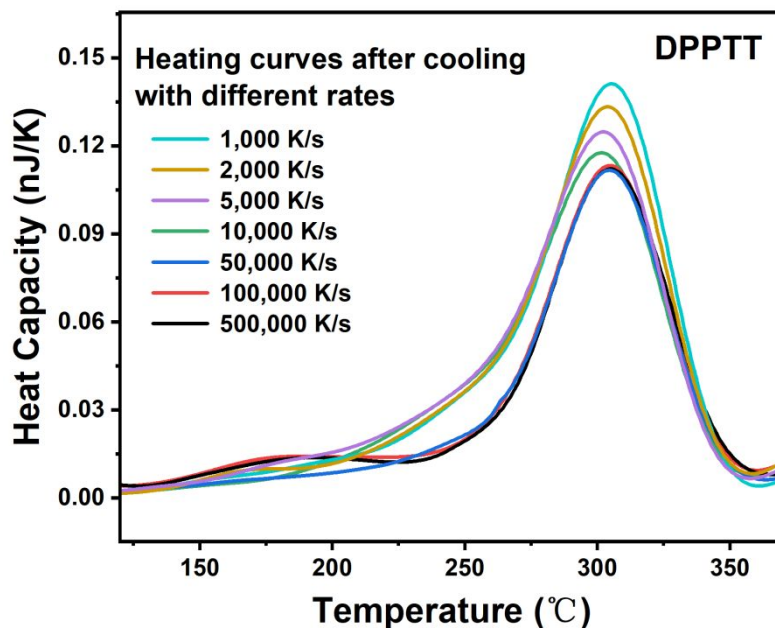


**Figure S1.** Reheating after cooling from the melt at different rates of DPPTT.

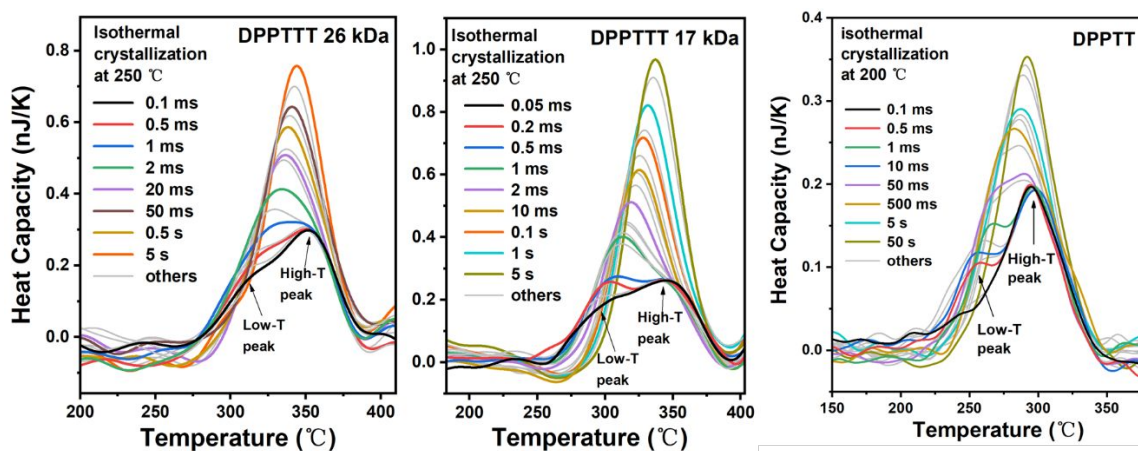


**Figure S2.** Reheating after isothermal crystallization at 250 °C of DPPTTT-26 kDa, DPPTTT-17 kDa and DPPTT samples.

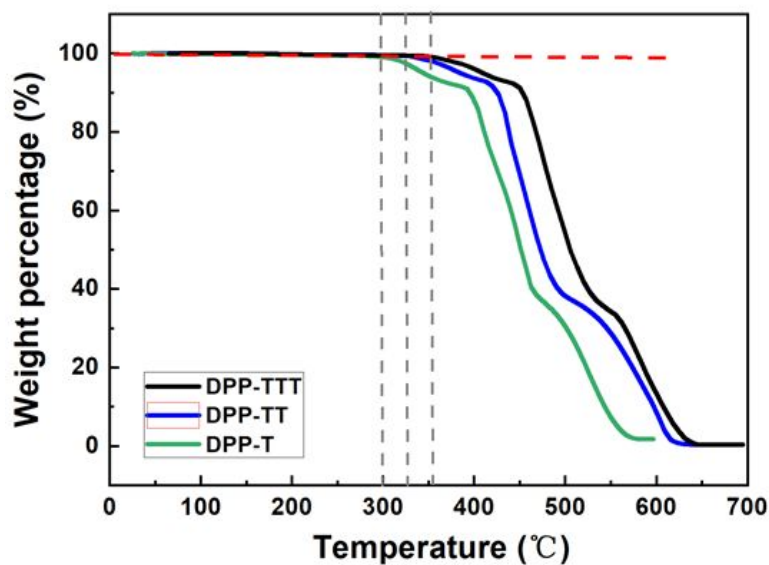


**Figure S3.** TGA heating curve of DPP-T, DPP-TT and DPP-TTT. TGA scans were carried out at a heating rate of 10 °C/minute. Obvious weight loss can be observed at around 300 °C for DPPT, 325 °C for DPPTT and 350 °C for DPPTTT. The highest isothermal temperature of each sample is set as 220 °C (DPPT), 270 °C (DPPT) and 320 °C (DPPT). They are both 30 °C lower than the degradation temperatures measured by TGA.

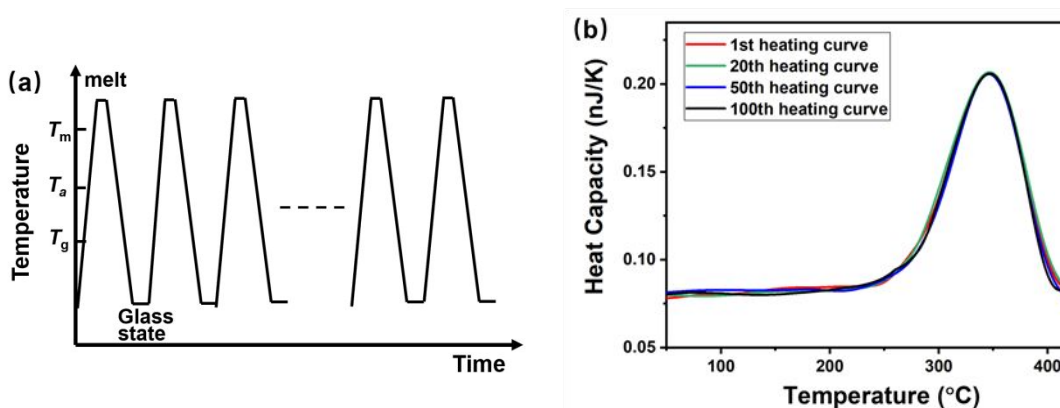


**Figure S4.** (a) Temperature-time program for repeating heating-cooling loops. All heating and cooling rate is 500,000 K/s. Waiting time at melt state is 0.05s. (b) The 1<sup>st</sup>, 20<sup>th</sup>, 50<sup>th</sup> and 100<sup>th</sup> heating curves of the heating-cooling loops. We repeat the heating-cooling loop for 100 times as shown in Figure R6, the 1<sup>st</sup>, 20<sup>th</sup>, 50<sup>th</sup> and 100<sup>th</sup> heating curves are almost overlap within the experimental error, indicating that the same enthalpy change at each thermal cycle.

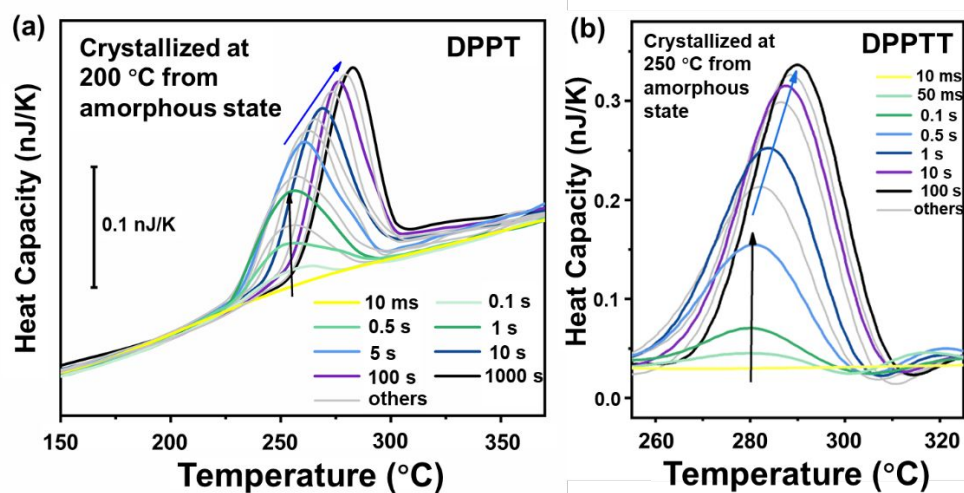


**Figure S5.** Reheating after isothermal crystallization from amorphous state (a) at 200 °C of DPPT and (b) at 250 °C of DPPTT.

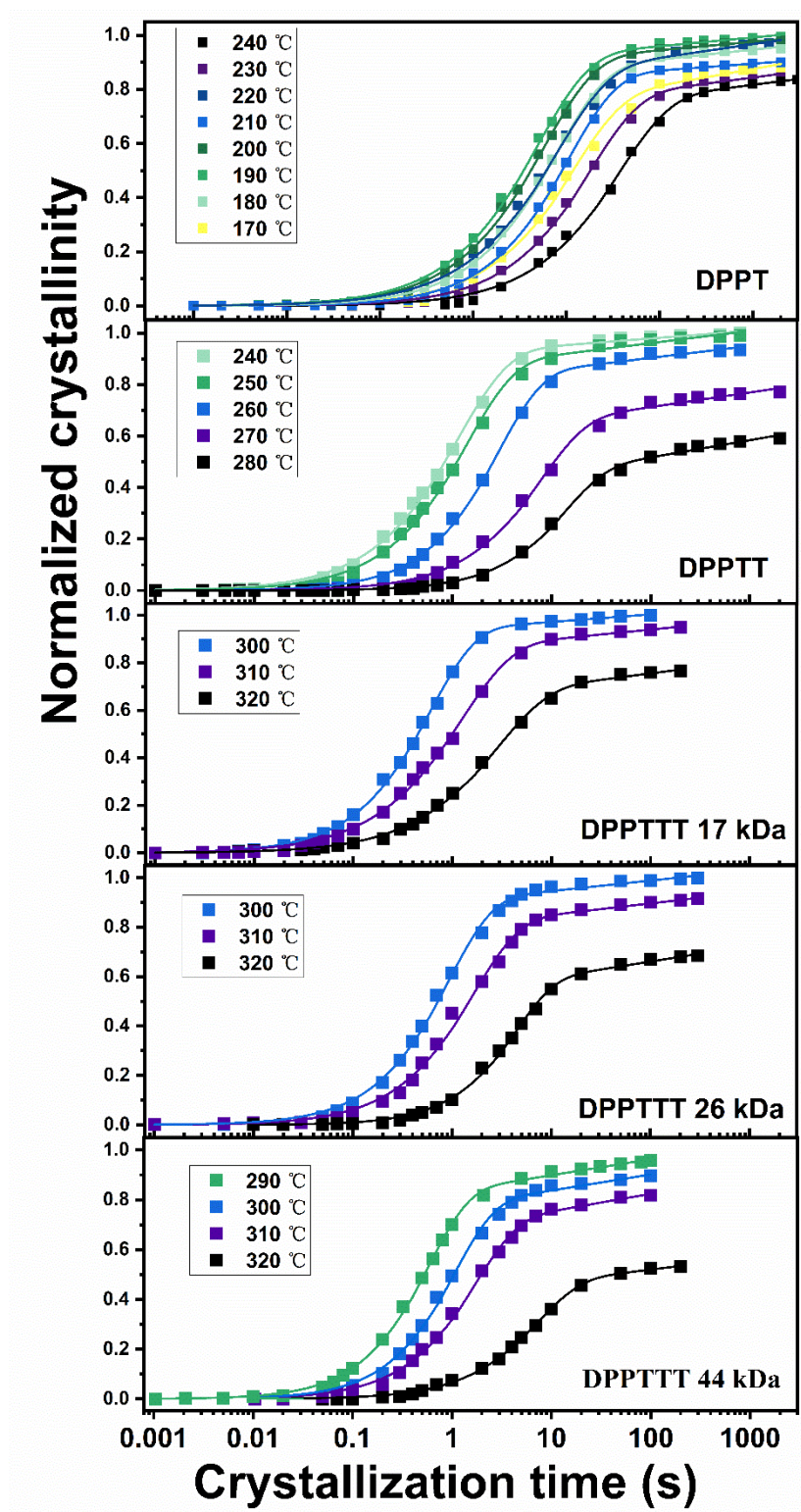


**Figure S6.** Normalized melting enthalpy (fraction of maximum crystallinity) on heating after isothermal crystallization from amorphous state at different temperatures of DPPT, DPPTT and DPPTTT samples.



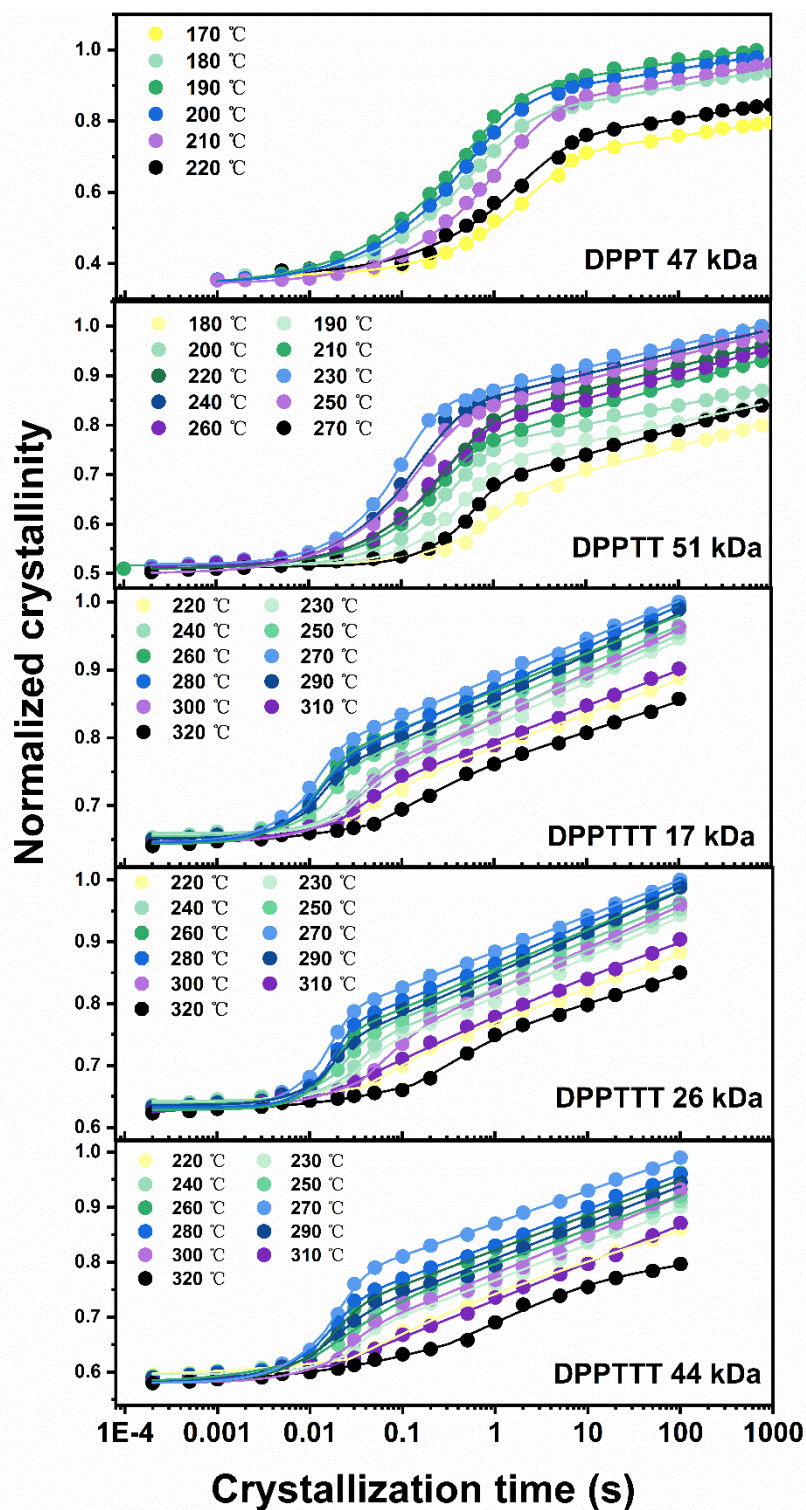


**Figure S7.** Normalized melting enthalpy change (fraction of maximum crystallinity) on heating after isothermal crystallization with crystals formed by fast kinetics at different temperatures of DPPT, DPPTT and DPPTTT samples.

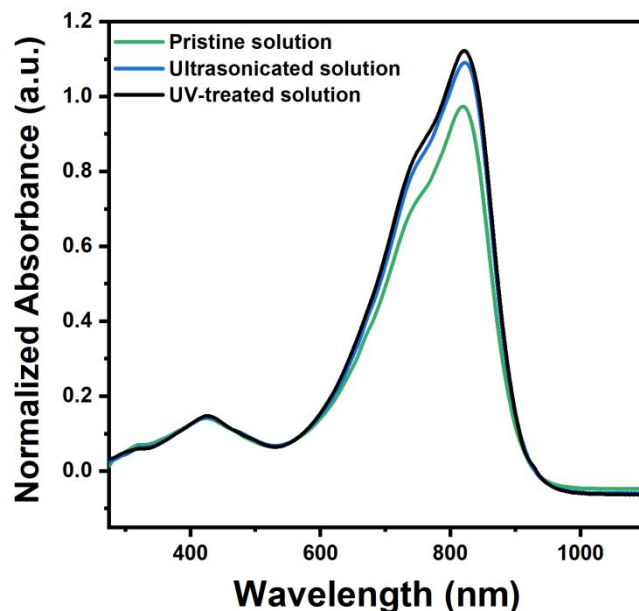


**Figure S8.** Normalized UV-vis absorption spectra of DPPTT solution with different pretreatments. Curves are normalized by the absorption peak centered at ca. 430 nm, which relates to the  $\pi$ - $\pi^*$  transition of isotropic amorphous chains in the solution.<sup>1,2</sup> Their charge transfer peak between 600 and 900 nm showed two distinct vibronic bands: the 0-1 (740 nm) and 0-0 (820 nm) transitions, which are attributed to the relative intra- and intermolecular coupling of delocalized excitons, arising from DPPTT self-assembly into aggregates.<sup>3, 4</sup> Therefore, the degree of polymer aggregation in solutions was estimated by the relative intensity of absorption peaks contributed by amorphous (430 nm) and aggregated states (600 and 900nm). The aggregates already exist in the pristine solution and become more or larger in the ultrasonicated and UV-treated solution.

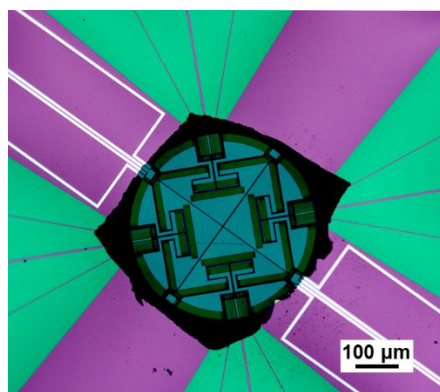


**Figure S9.** Sample image of DPPTT thin film on the Flash DSC sensor. To ensure the similar mass of each sample, the sample sizes are both controlled to just cover the heating area of the sensor. As the compared samples have the same mass, we compared the relative degree of crystallinity through the melting enthalpy (area of melting peak from the heat curves) of each sample.<sup>5</sup>



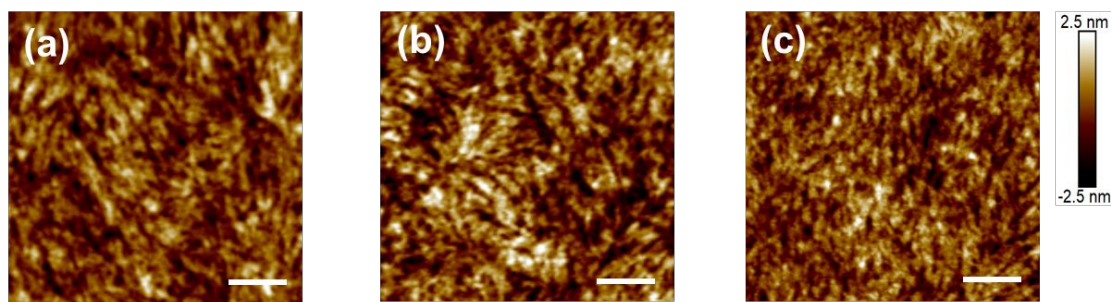


**Figure S10.** AFM images for DPPTT films spin coated from (a, b) ultrasonification pretreated solution and (c) UV irradiation pretreated solution. (a, c) are as-cast films, (b) is the annealed film. The scale bar indicates 200 nm.

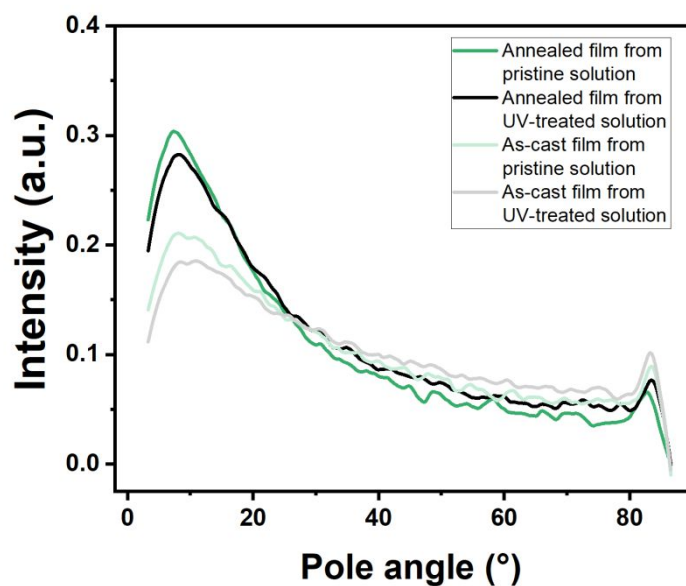


**Figure S11.** Pole figures for the (100) scattering peak for DPPTT film with different pre-treatments and post-thermal treatments. The intensity of (100) peak was normalized by exposure time, sample thickness and beam path length, later geometrically corrected orientation distribution function, or  $\sin(\chi)I(\chi)$ , was performed to obtain the relative orientation of the crystallite. The relative degree of crystallinity is obtained by integrating the area below each curve.

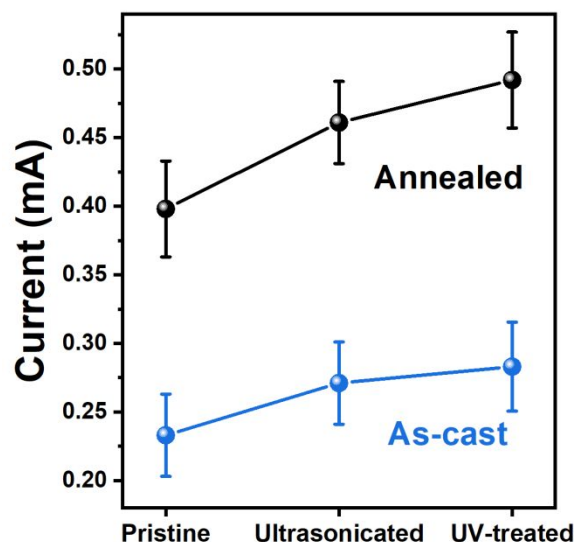


**Figure S12.** Average on current of DPPTT films with different pretreatments and post-annealing processes.

## References

1. Paquin, F.; Yamagata, H.; Hestand, N. J.; Sakowicz, M.; Bérubé, N.; Côté, M.; Reynolds, L. X.; Haque, S. A.; Stingelin, N.; Spano, F. C., Two-dimensional spatial coherence of excitons in semicrystalline polymeric semiconductors: Effect of molecular weight. *Physical Review B* **2013**, 88 (15), 155202.
2. McBride, M.; Persson, N.; Keane, D.; Bacardi, G.; Reichmanis, E.; Grover, M. A., A Polymer Blend Approach for Creation of Effective Conjugated Polymer Charge Transport Pathways. *ACS Appl Mater Interfaces* **2018**, 10 (42), 36464-36474.
3. Schroeder, B. C.; Kurosawa, T.; Fu, T.; Chiu, Y. C.; Mun, J.; Wang, G. J. N.; Gu, X.; Shaw, L.; Kneller, J. W.; Kreouzis, T., Taming charge transport in semiconducting polymers with branched alkyl side chains. *Adv. Funct. Mater.* **2017**, 27 (34), 1701973.
4. Ocheje, M. U.; Charron, B. P.; Cheng, Y.-H.; Chuang, C.-H.; Soldera, A.; Chiu, Y.-C.; Rondeau-Gagné, S., Amide-Containing Alkyl Chains in Conjugated Polymers: Effect on Self-Assembly and Electronic Properties. *Macromolecules* **2018**, 51 (4), 1336-1344.
5. Balko, J.; Rinscheid, A.; Wurm, A.; Schick, C.; Lohwasser, R. H.; Thelakkat, M.; Thurn-Albrecht, T., Crystallinity of poly(3-hexylthiophene) in thin films determined by fast scanning calorimetry. *J. Polym. Sci., Part B: Polym. Phys.* **2016**, 54 (18), 1791-1801.